Original Paper

Na+-Leak Channel, Non-Selective (NALCN) Regulates Myometrial Excitability and Facilitates Successful Parturition

Erin L. Reinl[a]   Peinan Zhao[b]   Wenjie Wu[a]   Xiaofeng Ma[a]   Chinwendu Amazu[a]
Rachael Bok[c]   K. Joseph Hurt[c]   Yong Wang[a]   Sarah K. England[a]

[a]Department of Obstetrics and Gynecology, Center for Reproductive Health Sciences, Washington University in St. Louis, School of Medicine, St. Louis, MO, [b]Department of Obstetrics and Gynecology, Washington University in St. Louis, School of Medicine, St. Louis, MO, [c]Department of Obstetrics & Gynecology, Divisions of Reproductive Sciences and Maternal Fetal Medicine, University of Colorado School of Medicine, Aurora, CO, USA

Abstract

Background/Aims: Uterine contractility is controlled by electrical signals generated by myometrial smooth muscle cells. Because aberrant electrical signaling may cause inefficient uterine contractions and poor reproductive outcomes, there is great interest in defining the ion channels that regulate uterine excitability. In human myometrium, the Na^+ leak channel, non-selective (NALCN) contributes to a gadolinium-sensitive, Na^+-dependent leak current. The aim of this study was to determine the role of NALCN in regulating uterine excitability and examine its involvement in parturition. ***Methods:*** Wildtype C57BL/6J mice underwent timed-mating and NALCN uterine expression was measured at several time points across pregnancy including pregnancy days 7, 10, 14, 18 and 19. Sharp electrode current clamp was used to measure uterine excitability at these same time points. To determine NALCN's contribution to myometrial excitability and pregnancy outcomes, we created smooth-muscle-specific NALCN knockout mice by crossing NALCN*fx/fx* mice with myosin heavy chain Cre (MHC*Cre-eGFP*) mice. Parturition outcomes were assessed by observation via surveillance video recording cre control, flox control, smNALCN*+/-*, and smNALCN*-/-* mice. Myometrial excitability was compared between pregnancy day 19 flox controls and smNALCN*-/-* mice. ***Results:*** We found that in the mouse uterus, NALCN protein levels were high early in pregnancy, decreased in mid and late pregnancy, and then increased in labor and postpartum. Sharp electrode current clamp recordings of mouse longitudinal myometrial samples from pregnancy days 7, 10, 14, 18, and 19 revealed day-dependent increases in burst duration and interval and decreases in spike density. NALCN smooth muscle knockout mice had reduced myometrial excitability exemplified by shortened action potential bursts, and an increased rate of abnormal labor,

Sarah K. England

Department of Obstetrics and Gynecology, Center for Reproductive Health Sciences
Washington University in St. Louis, School of Medicine, St. Louis, MO 63110, (USA)
Tel. (314) 286-1798, E-Mail englands@wustl.edu

KARGER

including prolonged and dysfunctional labor. ***Conclusions:*** Together, our findings demonstrate that the Na^+ conducting channel NALCN contributes to the myometrial action potential waveform and is important for successful labor outcomes.

Introduction

Uterine contractility is tightly regulated during pregnancy to ensure an appropriate length gestation (37–40 weeks in humans) and successful parturition. Throughout pregnancy, the uterus remains quiescent, producing only asynchronous, regional contractions that permit development of the growing fetus. At term, the uterus rapidly transitions to a state of activation, in which contractions increase in force, frequency, and synchrony to enable effective expulsion of the fetus. Excessive contractility (tachysystole) endangers both mother and fetus by increasing the risks for uterine rupture and fetal hypoxia due to insufficient placental perfusion [1, 2]. Conversely, insufficient contractility can lead to failure to progress through labor (labor dystocia), a principal indication for caesarean section [3, 4], which increases the risks of severe maternal morbidity and future placental abnormalities [5-7]. In the US, 32% of deliveries are by caesarean section, [8] a rate far in excess of the 10–15% rate recommended by the World Health Organization. To reduce the caesarean section rate, we must fully define the molecular and cellular mechanisms underlying normal labor, and specifically those that regulate contraction force and frequency.

Uterine contractions arise in response to the electrical activity of myometrial smooth muscle cells. Rhythmic depolarization and repolarization of the uterine myocyte membrane potential manifests as bursts of high-frequency electrical spikes. This electrical activity is closely coupled to contractile activity so that the amplitude, frequency, and duration of contractions correlate with the number of cells that are simultaneously active, their electrical burst frequency, and the duration of the bursts [9-12]. A key ion in the initiation of excitatory activity is calcium (Ca^{2+}). Upon spontaneous or agonist-mediated depolarization of the plasma membrane, activation of voltage-gated Ca^{2+} channels leads to influx of Ca^{2+}, which activates the contractile machinery. Bursts are terminated by activation of voltage-gated and Ca^{2+}-activated potassium (K^+) channels, which repolarize the plasma membrane and lead to muscle relaxation [13-15].

In addition to Ca^{2+} and K^+, sodium (Na^+) has long been considered an important ion in regulating myometrial excitability [16-19]. For example, the regenerative bursting properties of estrogen-treated, non-pregnant rat myometrium [17, 18] and of pregnant rabbit myometrium both rely on the presence of Na^+ [20]. Additionally, rat myometrial myocytes contain a Na^+-dependent leak current [21]. However, a role for Na^+ currents in the myometrium has been questioned because no work has clearly established the presence and identity of spontaneous currents that are sensitive to the Na^+-channel blocker tetrodotoxin [22-24].

To address the role for a Na^+ channel in human myometrial myocytes, we previously examined expression and activity of the sodium-activated leak channel non-selective (NALCN), a tetrodotoxin-*insensitive* member of the 4x6 transmembrane domain family of voltage-gated Ca^{2+} and Na^+ channels. Because NALCN lacks several charged residues in the putative voltage-sensing domain, this channel is voltage-insensitive and constitutively active [25]. The Na^+ leak activity of NALCN is essential for depolarizing the membrane potential, promoting spontaneous firing, and sustaining rhythmic burst activity in other spontaneously active cells [25-28]. We reported that NALCN is expressed in human myometrial myocytes and contributes to the leak current in myocytes from pregnant women [29]. Given these findings, we hypothesized that the Na^+ leak activity of NALCN increases myometrial excitability, and that this increase is essential for achieving successful parturition. Here, we tested this idea in a mouse model, and we report that NALCN expression in the myometrium is regulated throughout pregnancy and that this channel contributes to uterine excitability and functional labor.

KARGER

Materials and Methods

Mice

All animal procedures were carried out in accordance with the guidelines of care and use of animals set forth by the National Institutes of Health and were approved by the Animal Studies Committee at Washington University in St. Louis. Mice were kept on a 12 h light:dark cycle, with the light cycle from 6 am to 6 pm, and were fed standard Purina LabDiet PicoLab® Rodent Diet 20 chow. Wild-type C57BL/6J mice were obtained from Jackson Laboratory and bred in-house. *NALCN$^{fx/fx}$* mice were a kind gift from Dr. Dejian Ren at the University of Pennsylvania. These mice, bred on a C57BL/6J background, contain loxP sites flanking the fourth and fifth exons of NALCN. Excision results in an early termination codon before the fourth transmembrane domain of the first homologous repeat [27]. Female NALCN$^{fx/fx}$ mice were crossed with male mice expressing myosin heavy chain 11 promoter-driven Cre-eGFP (*smMHC$^{Cre-eGFP}$*) [30]. The male *NALCN$^{fx/WT}$ smMHC$^{Cre-eGFP/WT}$* F1 offspring were crossed to *NALCN$^{fx/fx}$* females to produce *NALCN$^{fx/fx}$ smMHC$^{Cre-eGFP/WT}$* (smNALCN$^{-/-}$), *NALCN$^{fx/WT}$ smMHC$^{Cre-eGFP/WT}$* (smNALCN$^{+/-}$), and *NALCN$^{fx/fx}$ smMHC$^{WT/WT}$* (flox control) F2 females that were used for parturition phenotyping. This breeding scheme was chosen because when carried by the female, Cre is expressed globally in oocytes and early *smMHC$^{Cre-eGFP}$* embryos, which could lead to global NALCN knockout. Cre is expressed during early spermatogenesis in *smMHC$^{Cre-eGFP}$* males, but its expression is lost before fertilization. Because of the embryonic expression of Cre, the flox control and smNALCN$^{-/-}$ females were all globally heterozygous for NALCN. Cre control mice (*smMHC$^{Cre-eGFP/WT}$*) used in parturition phenotyping were either F1 littermates or were the offspring of *smMHC$^{Cre-eGFP}$* males crossed with wild-type females.

For the experiment shown in Fig. 2D, E, primigravida C57BL/6 pregnant mice (10 hour mating encounter) were obtained from Charles River Laboratories on a protocol approved by the University of Colorado Institutional Animal Care and Use Committee. Gestation-age-matched mice on pregnancy day 19.5 were sacrificed in pairs: one actively laboring mouse (after delivery of the first pup) and one mouse not in labor (no vaginal bleeding). Other mice were allowed to deliver and sacrificed 24 hours postpartum. Uteri were removed to ice-cold PBS, opened longitudinally, cleaned of mesentery, fetal tissue, and membranes, and gently scraped to remove the endometrium before snap-freezing in liquid nitrogen. Samples were stored at -80 ºC until lysate preparation.

RNA Isolation and cDNA Synthesis

Total RNA was extracted from flash-frozen whole mouse uterine or brain tissue by using the Aurum Total RNA Fatty and Fibrous Tissue Pack Kit (BioRad, Hercules, CA), and cDNA was created by using the iScript cDNA Synthesis Kit (BioRad), both according to manufacturer's instructions.

Quantitative Real Time PCR (qRT-PCR)

After dissection, mouse uterine tissue was immediately transferred into a vial of RNA*later*® (Thermo Fisher Scientific, Waltham, MA) and stored at -20 °C. RNA was extracted as detailed above, and quality was confirmed by gel electrophoresis analysis of 28S to 18S rRNA ratio, and 260/280 nm and 260/230 nm absorbance ratios above 1.8 and 2.0, respectively. qRT-PCR reactions (20 µl) contained 5 pmol of each forward and reverse primer (for all online suppl. material, see www.karger.com/doi/10.1159/000491805, Suppl. Table S1), cDNA produced from 50 ng of RNA, and iQ SYBR Green Supermix (BioRad). Gene targets were amplified and quantified by the CFX96 BioRad Real-Time PCR Detection System. Temperature cycles were as follows: 95°C for 3 min, 40 cycles of (95°C for 10s, 57°C for 30s), and a 0.5°C increment melt curve from 65°C to 95°C. Primer efficiencies were ≥ 77% with mouse brain cDNA, and the calculated efficiency values were used in Pfaffl analysis of relative gene expression [31]. Target gene expression was normalized to the reference genes topoisomerase I (TOP1) and succinate dehydrogenase complex, subunit A (SDHA) and then averaged. These genes were chosen because of their stable expression in the myometrium across pregnancy [32].

Membrane Preparations

Flash-frozen mouse uterine or brain tissue was minced over ice and transferred to ice-cold membrane prep solution (250 mM sucrose, 50 mM MOPS, 2 mM EDTA, 2 mM EGTA, 1 mM PMSF, pH 7.4) containing cOmplete Mini EDTA-free Protease Inhibitor Cocktail (Roche, Indianapolis, IN). Tissue was homogenized

with the BioGen PRO200 homogenizer (ProScientific, Oxford CT) at 4 °C. Lysate was centrifuged at 14, 000 ×*g* for 15 min, and supernatants were transferred to ice-cold ultracentrifuge tubes. Samples were centrifuged at 100, 000 ×*g* for one hour. Pellets were resuspended in 1% Triton lysis buffer (150 mM NaCl, 10 mM Tris, 1% Triton X-100, pH 8.0) and rotated for two hours or overnight (no noticeable difference) at 4 °C. Non-solubilized protein was removed via centrifugation at 9000 ×*g* for 20 min at 4 °C.

Immunoblot

Protein concentrations of whole cell lysates and membrane preparations were measured by using a bicinchoninic acid protein assay kit (Pierce, Rockford, IL, USA). Protein samples were mixed with Laemmli sample buffer, heated to 65°C for 15 min, and stored at -20°C. Protein samples (40 µg each) were separated by 6% SDS-PAGE and transferred to a nitrocellulose membrane. After blocking in PBS containing 0.075% Tween-20 (PBST) and 5% milk, membranes were probed with the following primary antibodies: anti-NALCN N-20 (1:500; Santa Cruz Biotechnologies, Inc., Santa Cruz, CA, USA), anti-PDI (C81H6, Cell Signaling Technology, Danvers, MA), anti-GAPDH (1:1000; Millipore, Billerica, MA, USA), anti-transferrin receptor (1:1000; 84036 Abcam, Cambridge, UK), or anti-Na$^+$/K$^+$ ATPase α1 (1:500, sc-28800 Santa Cruz Biotechnologies, Inc.). Blots were then probed with HRP-conjugated secondary antibodies (1:4000; Jackson ImmunoResearch Laboratory Inc., West Grove, PA, USA) in PBST containing 3% milk. Signal was detected with Clarity ECL Western chemiluminescence (BioRad) and exposed onto film or viewed through a ChemiDoc MP Imaging System (BioRad). NALCN and Na$^+$/K$^+$-ATPase or PDI band pixel intensities were quantified using the gel analysis tool on ImageJ. Briefly, a flat line was drawn across the base of the intensity peak for each band to subtract background, and the area under the curve was quantified. NALCN values were normalized to the Na$^+$/K$^+$-ATPase or PDI values for each lane [33, 34]. Recently, it has been reported that Na$^+$/K$^+$-ATPase levels may change in the uterus across pregnancy, but the α1 subunit remains stable [35].

Histology

Protocol modified from BD Biosciences. Uterine tissue was isolated from six month-old smNALCN$^{-/-}$ and flox control non-pregnant mice and placed in a pre-labeled base mold filled with partially frozen optimal cutting temperature (OCT) medium over dry ice. The mold was then filled with OCT to cover the uterine tissue. The mold was then stored in -80°C freezer until ready for sectioning. 25µm sections were prepared on a cryostat, placed on cover glass and stored at -20°C until imaged. GFP was excited by 488 nm light and imaged on a Nikon Eclipse Ti-U Microscope with 2X/0.06 lens.

Current Clamp

Mice were sacrificed between 9:00 am and 11:00 am, their uteri were removed, and embryos were sacrificed. The uterus was dissected to obtain 1 cm by 0.5 cm strips of longitudinal muscle from all uterine regions, excluding the mesometrial border, in cold Kreb's buffer (133 mM NaCl, 4.7 mM KCl, 11.1 mM glucose, 1.2 mM MgSO$_4$, 1.2 mM KH$_2$PO$_4$, 1.2 mM CaCl$_2$, 10 mM TES free acid, pH to 7.4 with NaOH). Muscle strips were maintained in ice-cold Kreb's until experiments began (within six hours). For recordings, strips were pinned into a recording chamber on a Nikon Eclipse FN1 and superfused with warm (32 °C) Kreb's solution containing 5 µM wortmannin to inhibit contractions while maintaining spontaneous electrical activity. Sharp glass electrodes with tip resistances between 40 mΩ and 110 mΩ were filled with 2 M KCl and used to impale the tissue once contractions had arrested (usually within 15 minutes). Membrane potential was recorded at a 1 kHz sampling rate by using an Axon Multiclamp 700B amplifier and Axon Digidata 1550. Data were recorded through the pCLAMP 10.4 software. Burst duration (time between first and last spike), burst interval (time between last spike of the previous burst and first spike of the next burst), and spikes per burst were analyzed with a customized Matlab program on Matlab R2015b. In this program, the 'find peaks' function was modified to identify voltage spikes without the need to adjust for changes in baseline or reduce noise. Spikes were defined as those having a minimum prominence of 7 mV and a minimum width of 20 ms. Clusters of spikes, or bursts, were defined as those having a minimum duration of 2000 ms and a minimum interval of 4000 ms. The number of intervals or bursts differed in each recording depending on whether a given recording started or ended with an interval or burst. Bursts and intervals were recorded until the electrode dislodged or became loose from the tissue. Recordings ranged in duration from 9s (one burst) to 16 min.

KARGER

Cellular Physiology and Biochemistry

Cell Physiol Biochem 2018;48:503-515

DOI: 10.1159/000491805
Published online: July 17, 2018

© 2018 The Author(s). Published by S. Karger AG, Basel
www.karger.com/cpb

507

Reinl et al.: NALCN in Mouse Myometrial Excitability and Parturition

Parturition Phenotyping

Cre control, flox control, smNALCN$^{+/-}$, and smNALCN$^{-/-}$ nulliparous female mice between the ages of seven weeks and six months were mated with WT C57BL/6J males ages eight weeks to eleven months, for two hours between 2:30 pm and 5:30 pm. At the end of the two-hour period, females with a copulation plug were defined as pregnant on pregnancy day 0 (P0). On P17 or P18, females were placed in individual cages in front of D-Link DCS-932L surveillance cameras (Taipei, Taiwan). Cameras capturing one frame/second began recording at 7:00 pm on P18 and were stopped after delivery was completed or when the female was sacrificed. The timing of delivery of each pup was manually recorded from the videos. Gestation length was defined as the length of time between detection of the copulation plug on P0 (about 5:30 pm) and delivery of the first pup. Duration of labor was defined as the length of time between the delivery of the first and last pups, and average pup interval was calculated by dividing the total labor duration by one less than the total number of pups delivered. Prolonged labor was defined as labor with one or more pup interval longer than 62 min (> 95th percentile). Delayed labor was defined as delivery of the first pup occurring later than 495 hours (20.63 days) post-conception (> 95th percentile). Dysfunctional labor was defined as the incomplete delivery of a full litter by morning of day 22 (P21.75). Dams experiencing dysfunctional labor were sacrificed by P21.75 because of discomfort. Litter size included all live or dead pups or embryos at term or at P19; early pregnancy fetal demises (*in utero* clots) were not counted. Pups were weighed within 24 hours of birth.

Staging Diestrus

Mice in the diestrus stage of the estrus cycle were identified as previously described [36]. Briefly, between 2:00 pm and 4:00 pm daily, DPBS vaginal lavages were performed and streaked onto glass slides. Slides were stained with Crystal Violet (Sigma-Aldrich, St. Louis, MO) and visualized on a Leica ICC50 upright microscope. Lavages consisting primarily of leukocytes were considered to be from females in diestrus. Females in diestrus were sacrificed between 3:30 and 5:00 pm, and their uteri were removed and flash frozen.

Statistical Analysis

Data comparing more than one group with one dependent variable were analyzed using Kruskal-Wallis one-way ANOVA, not assuming a normal distribution. Individual differences were further assessed by Dunn's multiple comparisons test. The generalized linear model was conducted to estimate the daily changing trend with myometrial excitability parameters. In the generalized linear model, the Least Squares mean for the daily effect was constructed for the pairwise comparisons of electrophysiology parameters of WT mouse uterus across different stages. The generalized linear model was also performed for the flox control vs. smNALCN$^{-/-}$ sharp electrode analysis. Wilcoxon rank sum test was performed on the data obtained from the immunoblot analysis. Fisher's exact test was conducted to test the abnormal labor proportions, and Chi square analysis was performed to compare Kaplan-Meier plots. GraphPad Prism 6 (San Diego, CA, USA) software and SAS (version 9.3, SAS institution Inc., Cary, NC, USA) were used for statistical calculations.

Results

Myometrial Excitability Throughout Pregnancy

To assess the myometrial electrical bursting activity throughout mouse pregnancy, we performed sharp electrode current clamp experiments on mouse uterine longitudinal muscle from different stages of pregnancy. Regenerative spontaneous bursting activity was measured in myometrial samples at five stages of pregnancy: pregnancy days 7, 10, 14, 18, and 19 (P7, P10, P14, P18, and P19). We analyzed four parameters: burst interval, burst duration, spike number, and spike density, which correlate with the frequency, duration, and strength of uterine contraction. We used a generalized linear model to analyze the progressive daily effect of pregnancy on each of these parameters using day 7 as baseline (the first pregnancy time point tested) (Table 1). This model accounts for the individual variance between mice. Burst interval (Fig. 1b), duration (Fig. 1c), and spikes per burst (Fig. 1d) showed significant increases throughout pregnancy, whereas the spike density significantly decreased (Fig. 1e) (Table 1).

KARGER

Cellular Physiology and Biochemistry

Cell Physiol Biochem 2018;48:503-515

DOI: 10.1159/000491805
Published online: July 17, 2018

© 2018 The Author(s). Published by S. Karger AG, Basel
www.karger.com/cpb

508

Reinl et al.: NALCN in Mouse Myometrial Excitability and Parturition

NALCN Expression in the Mouse Uterus

Recent studies have shown that NALCN contributes to sustained depolarization and spike trains in interstitial cells of Cajal and hermaphrodite-specific neurons in *C. elegans* [28, 37]. Our laboratory also demonstrated that NALCN contributes to the leak current in human myometrium [29]. To determine whether *Nalcn* mRNA is expressed in the mouse uterus, we initially isolated uterine tissue from different stages of pregnancy and performed quantitative real-time PCR. We found a trend in the effect of gestational timing on *Nalcn* mRNA levels (P = 0.08) with expression levels being higher in NP and at P10 than at P14, P18, and P19 (Fig. 2a). Western blot analysis showed that uterine cell membranes from early pregnant (P7 and P10) mice contained significantly more NALCN protein than did those from P14, P18, and P19 mice (Fig. 2b and c). Western blot analysis of uterine tissue from a separate group of mice showed that uteri from laboring mice had higher levels of NALCN than did gestation-age-matched non-laboring mice, although this was not significant. However, NALCN levels were significantly elevated in postpartum day 1 mice (Fig. 2d and e). Together, these findings indicate that NALCN levels in the uterus decrease in mid-pregnancy and then increase at labor and remain high in the early postpartum period.

NALCN Smooth Muscle Knockout Mice

Qualitatively, we observed an inverse correlation between burst interval and the levels of NALCN protein at time points throughout pregnancy; when burst intervals (Fig. 1b) were short, NALCN levels were high (Fig. 2c), and vice versa. To better define NALCN's role in modulating burst activity and its effects on pregnancy outcomes, we created a smooth-muscle-specific NALCN knockout mouse. We crossed the myosin heavy chain-11 promoter-driven Cre-IRES-eGFP mouse (*smMHC^Cre-eGFP*) with a *NALCN^fx/fx* mouse to create smNALCN^-/- mice (Fig. 3a) [27, 30]. We

Table 1. Mixed model analysis of pregnancy day effect in electrophysiology parameters. s, seconds

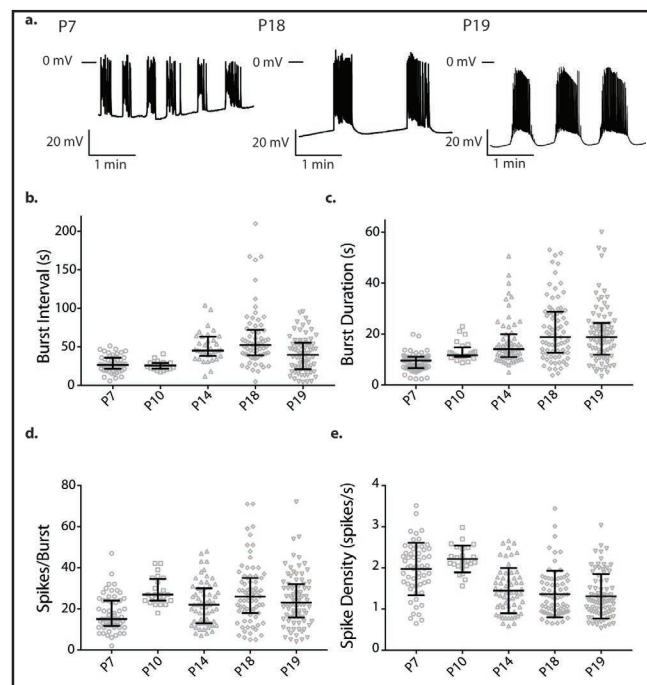| Parameter	Value	P-value
Interval (s)		
Baseline	27.98 ± 5.52 s	
Daily change	1.97 ± 0.36 s	< 0.0001
Duration (s)		
Baseline	9.63 ± 1.90 s	
Daily change	0.99 ± 0.12 s	< 0.0001
Spikes/Burst		
Baseline	19.85 ± 2.33	
Daily change	0.53 ± 0.15	0.001
Spike Density (spikes/s)		
Baseline	2.04 ± 0.11 spikes/s	
Daily change	-0.063 ± 0.007 spikes/s	< 0.0001

Fig. 1. Myometrial excitability throughout pregnancy. a) Representative myometrial membrane potential traces from P7, P18, and P19 mice. b–e) Average burst interval (b), burst duration (c), spikes per burst (d), and spike density (e) from the indicated pregnancy time points. Data points represent the respective values from each burst or interval recorded, the lines represent the median and interquartile range. Burst interval P7 n = 51 (6 mice), P10 n = 19 (3 mice), P14 n = 35 (7 mice), P18 n = 66 (7 mice), P19 n = 70 (6 mice). Burst duration, spikes/burst, and spike density P7 n = 58 (6 mice), P10 n = 24 (3 mice), P14 n = 59 (7 mice), P18 n = 75 (7 mice), P19 n = 82 (6 mice).

Cellular Physiology and Biochemistry

Cell Physiol Biochem 2018;48:503-515

DOI: 10.1159/000491805
Published online: July 17, 2018

© 2018 The Author(s). Published by S. Karger AG, Basel
www.karger.com/cpb

509

Reinl et al.: NALCN in Mouse Myometrial Excitability and Parturition

selected a smooth-muscle-specific Cre [38] to avoid any contribution of brain or gonadal NALCN expression. Additionally, *Nalcn* mutations have not been linked with other smooth muscle pathologies, namely vascular or severe gastrointestinal phenotypes, and thus we did not anticipate any non-reproductive effects in smNALCN$^{-/-}$ mice. To confirm this, we measured carotid artery compliance, aorta compliance, and blood pressure; all were similar between flox control and smNALCN$^{-/-}$ males (see online suppl. material, Suppl. Fig. S1).

To assess efficiency of NALCN knockout in the smNALCN$^{-/-}$ mouse uteri, we performed Western blot analysis of NALCN in whole uterine membrane preparations from non-pregnant mice in the diestrus stage. Many uteri had reduced NALCN protein (Fig. 3b). However, the average levels of both NALCN protein (Fig. 3c) were similar between knockouts and controls. We considered two possible explanations for this finding. First, NALCN may be expressed in the tissues besides the smooth muscle, including the endometrium, decidua and the stroma. Indeed, NALCN protein was present in the endometrium and stroma in the human protein atlas (http://www.proteinatlas.org/). Also, immunoblot analysis of decidual tissue verified that non-muscle cells within the uterus express NALCN (see online suppl. material, Suppl. Fig. S2). However, histology demonstrated that GFP (which marks the Cre-expressing cells) was expressed predominantly in the myometrium (Fig. 3d), indicating that Cre-recombination of *Nalcn* should not have occurred in the endometrium.
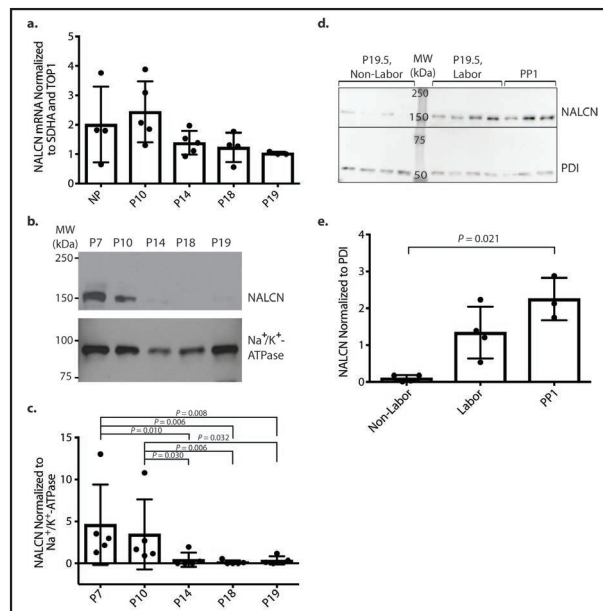

Fig. 2. NALCN expression in the uterus throughout pregnancy and post-partum. a) qRT-PCR of NALCN mRNA in the mouse uterus across pregnancy. TOP1 and SDHA were used as standards for quantification. No significant differences were observed by Kruskal-Wallis one-way ANOVA with Dunn's correction for multiple comparisons. b) Representative western blot of NALCN protein levels across pregnancy in the mouse uterus. The membrane protein, protein disulfide-isomerase (PDI) served as the loading control. c) Quantification of NALCN protein levels in mouse uterine membrane preparations from across pregnancy. NALCN levels were normalized to the Na$^+$/K$^+$-ATPase loading control. Statistical analysis by the Wilcoxon rank sum test. d) Western blot of NALCN from uterine membrane preparations from mice matched for term labor and non-labor, and at post-partum day 1 (PP1). e) Quantification of NALCN levels from western blot in (d). Statistical analysis by Kruskal-Wallis one-way ANOVA with Dunn's correction for multiple comparisons. In c and e, mean values and standard deviations are presented.

Parturition Defects in smNALCN$^{-/-}$ Mice

Although Na$^+$ currents have been detected in the myometrium, the role they play in parturition was unknown. To determine whether NALCN is required for normal labor, we mated flox control, Cre control, smNALCN$^{+/-}$, and smNALCN$^{-/-}$ females to wild-type males for two hours and then followed those that had a copulation plug. The transgenic dams were healthy throughout pregnancy and did not display any obvious phenotypes. Beginning on P18, we used a surveillance camera to continuously observe the pregnant mice until delivery. Both Flox and Cre control mice had ~20% abnormal labors, which can occur in the first parity. However, in comparison, smNALCN$^{-/-}$ and smNALCN$^{+/-}$ dams experienced a higher rate of abnormal labor of 40 and 60%, respectively. Abnormal labors consisted

510

Fig. 3. Development of the smNALCN$^{-/-}$ mouse. a) Breeding strategy. b) Representative western blot of NALCN in uteri from diestrus flox control and smNALCN$^{-/-}$ mice. The GFP blot was run separately but from the same samples. c) Relative quantification of NALCN protein levels normalized to PDI. Error bars represent standard deviation. d) Bright field image of NP smNALCN$^{-/-}$ and flox control uterine cross sections illuminated with 488 nm. Myometrium layer (Myo), endometrium layers (endo), and uterine lumen are labeled.

Fig. 4. Parturition outcomes in smNALCN$^{-/-}$ mice. a) Rates of abnormal vs. normal labor in each genotype. Fisher's exact test was performed on the number of dams, not the percentages, and the P-value was equal to 0.041. Flox control n = 15, Cre control n = 13, smNALCN$^{+/-}$ n = 10, smNALCN$^{-/-}$ n = 15. b) Kaplan-Meier curve denoting the time to completion of delivery. Dams that underwent dysfunctional labor are marked as black arrows and were classified as 'lost to follow-up.' P-value is 0.068 across all groups. c) Correlation between labor duration and litter size. Pearson correlation P-value is 0.0011. d) Correlation between gestation length and litter size. Pearson correlation P-value is 0.0122.

KARGER

of prolongation of labor (labor with one or more pup interval longer than 62 min (> 95th percentile), delayed labor (delivery of the first pup occurring later than 495 hours (20.63 days) post-conception (> 95th percentile), or dysfunctional parturition (incomplete delivery of the full litter by P21.75) (Fig. 4a). We used Kaplan-Meier analysis to assess the duration of pregnancy from P18 until completion of delivery and found that smNALCN$^{-/-}$ mice took longer than the controls to deliver, but this difference was not significant ($P = 0.068$) (Fig. 4b). A more detailed analysis of parturition in each animal indicated that the average length of time from copulation to the time of delivery of the first pup (gestation length) did not differ significantly between the four genotypes, nor did the duration in labor (Table 2). Notably, smNALCN$^{+/-}$ and smNALCN$^{-/-}$ dams spent similar lengths of time in labor as flox controls, despite having significantly smaller litter sizes (Table 2). Because litter size is proportional to the labor duration (Fig. 4c), we accounted for differences in litter size by measuring the average time between delivery of each pup (mean pup interval), and found this was significantly longer for smNALCN$^{-/-}$ and smNALCN$^{+/-}$ dams than for the flox controls (Table 2). Although mean gestation length did not significantly differ between groups, the number of pups per litter negatively correlated with gestation length in smNALCN$^{-/-}$ females, in that smaller litters delivered later (Fig. 4d). In addition to smaller litters, smNALCN$^{-/-}$ dams had larger pups than flox controls (see online suppl. material, Suppl. Fig. S3). Together, these data indicate that NALCN contributes to efficient parturition and normal litter size in mice.

Reduced Uterine Excitability in smNALCN$^{-/-}$ Mice

To determine the mechanism by which NALCN contributes to parturition, we used sharp electrode current clamp to compare myometrial excitability in smNALCN$^{-/-}$ and flox control dams at P19 (Fig. 5a). We did not detect a difference in burst interval (Fig. 5b), however burst duration and the number of spikes/burst were significantly lower in smNALCN$^{-/-}$ myometrium than in flox controls (Fig. 5c and d). Spike density was similar between the smNALCN$^{-/-}$ and the flox controls (Fig. 5e). Given the sharp electrode data and the high rate of parturition defect, we conclude that NALCN is important for sustaining burst duration in the myometrium and is necessary for successful delivery.

Table 2. Pregnancy and parturition parameters. P-values determined by Kruskal-Wallis one-way ANOVA. * P < 0.05, ** P < 0.01 for Dunn's multiple comparisons test against flox controls. ^{a}n values are larger for mean gestation length than mean pup interval and mean labor duration because the latter two measures exclude dams that could not deliver more than one pup. n values are larger for mean litter size because they include dams that could not deliver even one pup and those sacrificed at P19 for sharp electrode experiments

Measure	Flox Control	Cre Control	smNALCN$^{+/-}$	smNALCN$^{-/-}$	P-value
Mean Gestation Length, days ± SEM (n)^a	19.47 ± 0.13 (15)	19.63 ± 0.13 (12)	19.53 ± 0.20 (10)	19.89 ± 0.13 (14)	0.323
Mean Litter Size, no. pups ± SEM (n)	6.9 ± 0.35 (19)	6.4 ± 0.31 (13)	4.9 ± 0.57* (10)	4.6 ± 0.47** (25)	0.003
Mean Pup Interval, min ± SEM (n)	16.4 ± 1.3 (14)	25.6 ± 6.3 (12)	37.8 ± 13.9* (10)	27.6 ± 3.9* (12)	0.030
Mean Labor Duration, min ± SEM (n)	92.0 ± 8.3 (14)	131.0 ± 26.1 (12)	104.0 ± 13.6 (10)	87.8 ± 15.7 (12)	0.610

Cellular Physiology and Biochemistry

Cell Physiol Biochem 2018;48:503-515

DOI: 10.1159/000491805
Published online: July 17, 2018

© 2018 The Author(s). Published by S. Karger AG, Basel
www.karger.com/cpb

512

Reinl et al.: NALCN in Mouse Myometrial Excitability and Parturition

Discussion

Previously, we showed that NALCN is expressed in human myometrial myocytes and contributes to the Na+ leak current in these cells [29]. Here, we present evidence that NALCN is important in uterine physiology during pregnancy and parturition in mice. We report that NALCN expression in the mouse uterus varies across pregnancy and is critical for successful labor. Specifically, smooth-muscle NALCN knockout mice had an increased incidence of abnormal labor and reduced uterine excitability. Our study supports the findings of others that Na+ plays an important role in uterine excitability [17-19] and emphasizes that even subtle changes in ion currents in the myometrium can have a large impact on reproductive success. Although abnormal parturition was reported in a transgenic mouse overexpressing the

Fig. 5. Myometrial excitability in smNALCN$^{-/-}$ uterus. a) Representative membrane potential traces from P19 flox control and smNALCN$^{-/-}$ longitudinal muscle. b – e) Average burst interval, burst duration, number of spikes per burst, and spike density comparison in flox control and smNALCN$^{-/-}$ longitudinal myometrium. Data points represent the respective values from each burst or interval recorded, the lines represent the median and interquartile range. b) Burst interval of flox control n = 38 (5 mice), and smNALCN$^{-/-}$ n = 58 (6 mice). c – e) Burst duration, spikes/burst, and spike density of flox control n = 31 (5 mice), and smNALCN$^{-/-}$ n = 51 (8 mice).

calcium-activated potassium channel KCa2.3, to our knowledge, this is the first report of abnormal labor occurring in an animal lacking a particular ion channel.

Our observation that burst interval in myometrium from wild-type mice inversely correlated with NALCN expression level was consistent with the established ability of NALCN to increase spontaneous firing [25-27]. Thus, we anticipated that smNALCN$^{-/-}$ P19 myometrium would have a prolonged burst interval, but this was not the case. Instead, we observed no significant differences in myometrial burst interval or spike density between smNALCN$^{-/-}$ and flox controls. However, we found that smNALCN$^{-/-}$ myometrium had shorter burst durations and fewer spikes per burst than flox controls. Our finding that NALCN contributed to burst duration corroborates other studies showing that NALCN contributes to sustained depolarization and spike trains in interstitial cells of Cajal in mice and hermaphrodite-specific neurons in *C. elegans* [28, 37]. One possible explanation for why NALCN did not appear to regulate burst interval is that NALCN protein was expressed at a low level at P19 before labor; NALCN may contribute more to regulating burst interval in myometrium from stages with higher NALCN expression, such as in labor, at P7, or at P10. Additionally, multiple ion channels regulate myometrial excitability, many of which are differentially regulated throughout pregnancy, and NALCN current is likely to be affected by changes in the activity of other channels.

Our findings that smNALCN$^{-/-}$ females had a higher rate of abnormal labor, longer pup delivery intervals, and shorter burst durations in the myometrium than controls suggest that these mice had insufficient uterine activity to efficiently deliver their pups. Although none of the individual classifications of abnormal labor (delayed, prolonged, or dysfunctional) were significantly different between the genotypes studied, the smNALCN$^{-/-}$ females were at increased risk of extreme or pathological labor outcomes. Notably, three out of the five mice that experienced dysfunctional labor were able to deliver at least one pup, indicating
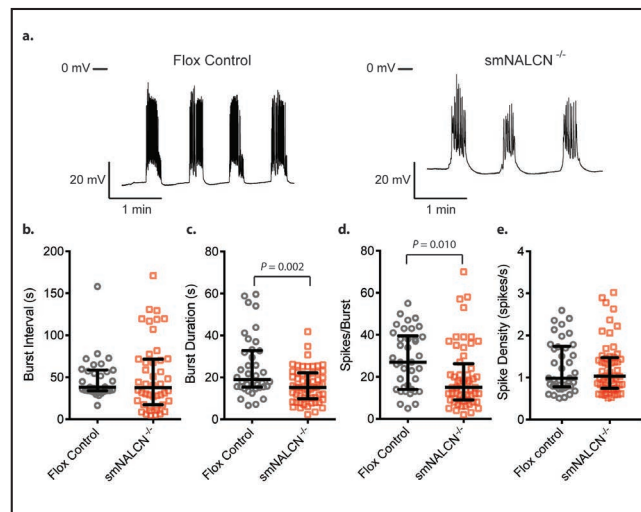
Cellular Physiology and Biochemistry

Cell Physiol Biochem 2018;48:503-515

DOI: 10.1159/000491805
Published online: July 17, 2018

© 2018 The Author(s). Published by S. Karger AG, Basel
www.karger.com/cpb

513

Reinl et al.: NALCN in Mouse Myometrial Excitability and Parturition

that these dams had undergone cervical ripening but were unable to produce the sustained contractions needed to expel the later offspring. A more subtle but similar effect of reduced contractility was suggested by the prolonged average pup intervals in smNALCN⁻/⁻ and smNALCN⁺/⁻ dams. Additionally, the greater proportion of smNALCN⁻/⁻ dams with delayed labor outcomes was likely due, in part, to their smaller litter size. At this time, we do not know why these mice had smaller litters than the other genotypes. We did not detect blood pressure or vascular abnormalities in smNALCN⁻/⁻ males, suggesting that the small litter size was not due to vascular changes, but future studies are needed to assess cardiovascular health in pregnant smNALCN⁻/⁻ females. We also noted a larger average pup weight in the smNALCN⁻/⁻ mice, which may have occurred because of the slightly longer time *in utero* and the smaller litter size. Future studies should explore why loss of NALCN leads to reduced litter size.

We observed dynamic regulation of uterine NALCN levels throughout pregnancy and into the postpartum period, supporting the notion that NALCN is important for uterine function. The observed NALCN expression pattern suggests that NALCN protein levels are negatively regulated by progesterone, the master coordinator of pregnancy [39]. NALCN levels increased at labor and into the postpartum period, in a fashion similar to contraction-associated proteins [23]. These proteins shift the uterus from the quiescent non-laboring state characterized by stochastic, asynchronous contractions to the activated laboring state, characterized by synchronous and forceful contractions. NALCN expression was high in the post-partum uteri, perhaps indicating that NALCN is responsible for the increased uterine tone needed to prevent postpartum hemorrhage and blood loss. However, smNALCN⁻/⁻ mice did not exhibit excessive blood loss post-delivery.

Our observation that NALCN was expressed at a high level in the uterus in early pregnancy, when the uterus is quiescent and myocytes are electrically uncoupled, leads us to speculate about the function of NALCN at this time. In early pregnancy, uterine myocytes undergo rapid hyperplasia [40], which could require depolarizing currents produced by NALCN [41]. Although we did not observe an obvious defect in uterine hyperplasia in smNALCN⁻/⁻ mice, compensatory mechanisms could have sustained proliferation. Another possibility is that NALCN, which functions in osmoregulation [42], acts with the epithelial sodium channel and the cystic fibrosis transmembrane conductance regulator channel in the endometrium to regulate luminal fluid levels and thereby plays a role in embryo implantation [43]. Indeed, this potential role for NALCN may be why smNALCN⁻/⁻ dams show reduced litter sizes. Although we did not assess NALCN expression in all uterine compartments, our observation that NALCN knockdown was incomplete in smNALCN⁻/⁻ mice in conjunction with evidence of its presence in the decidua suggests that NALCN is expressed in the endometrium. Layer-specific identification of NALCN expression levels and localization will be prohibitive until immunohistochemistry compatible NALCN antibodies are produced.

In summary, our study established a novel role for the Na⁺ channel NALCN in sustaining myometrial burst duration and regulating myometrial excitability and labor efficiency. Future work could lead to the development of therapies to increase NALCN activity, which could be used to treat labor dystocia and thereby help decrease the rate of cesarean sections.

Acknowledgements

KARGER

Cellular Physiology and Biochemistry

Cell Physiol Biochem 2018;48:503-515

DOI: 10.1159/000491805
Published online: July 17, 2018

© 2018 The Author(s). Published by S. Karger AG, Basel
www.karger.com/cpb

514

Reinl et al.: NALCN in Mouse Myometrial Excitability and Parturition

Disclosure Statement

The authors have no competing financial interests to report.

References

1 Heuser CC, Knight S, Esplin MS, Eller AG, Holmgren CM, Manuck TA, Richards D, Henry E, Jackson GM: Tachysystole in term labor: incidence, risk factors, outcomes, and effect on fetal heart tracings. Am J Obstet Gynecol 2013;209:32 e31-36.

2 Sheiner E, Levy A, Ofir K, Hadar A, Shoham-Vardi I, Hallak M, Katz M, Mazor M: Changes in fetal heart rate and uterine patterns associated with uterine rupture. J Reprod Med 2004;49:373-378.

3 Gifford DS, Morton SC, Fiske M, Keesey J, Keeler E, Kahn KL: Lack of progress in labor as a reason for cesarean. Obstet Gynecol 2000;95:589-595.

4 Barber EL, Lundsberg LS, Belanger K, Pettker CM, Funai EF, Illuzzi JL: Indications contributing to the increasing cesarean delivery rate. Obstet Gynecol 2011;118:29-38.

5 Liu S, Liston RM, Joseph KS, Heaman M, Sauve R, Kramer MS, Maternal Health Study Group of the Canadian Perinatal Surveillance S: Maternal mortality and severe morbidity associated with low-risk planned cesarean delivery versus planned vaginal delivery at term. CMAJ 2007;176:455-460.

6 Silver RM, Landon MB, Rouse DJ, Leveno KJ, Spong CY, Thom EA, Moawad AH, Caritis SN, Harper M, Wapner RJ, Sorokin Y, Miodovnik M, Carpenter M, Peaceman AM, O'Sullivan MJ, Sibai B, Langer O, Thorp JM, Ramin SM, Mercer BM, National Institute of Child H, Human Development Maternal-Fetal Medicine Units N: Maternal morbidity associated with multiple repeat cesarean deliveries. Obstet Gynecol 2006;107:1226-1232.

7 Clark SL, Belfort MA, Dildy GA, Herbst MA, Meyers JA, Hankins GD: Maternal death in the 21st century: causes, prevention, and relationship to cesarean delivery. Am J Obstet Gynecol 2008;199:36 e31-35; discussion 91-32 e37-11.

8 Hamilton BE, Martin JA, Osterman MJ, Curtin SC, Matthews TJ: Births: Final Data for 2014. Natl Vital Stat Rep 2015;64:1-64.

9 Marshall JM: Regulation of activity in uterine smooth muscle. Physiol Rev Suppl 1962;5:213-227.

10 Parkington HC, Coleman HA: Ionic mechanisms underlying action potentials in myometrium. Clin Exp Pharmacol Physiol 1988;15:657-665.

11 Lammers WJ: The electrical activities of the uterus during pregnancy. Reprod Sci 2013;20:182-189.

12 Wray S: Insights from physiology into myometrial function and dysfunction. Exp Physiol 2015;100:1468-1476.

13 Aguilar HN, Mitchell BF: Physiological pathways and molecular mechanisms regulating uterine contractility. Hum Reprod Update 2010;16:725-744.

14 Wang SY, Yoshino M, Sui JL, Wakui M, Kao PN, Kao CY: Potassium currents in freshly dissociated uterine myocytes from nonpregnant and late-pregnant rats. J Gen Physiol 1998;112:737-756.

15 Brainard AM, Korovkina VP, England SK: Potassium channels and uterine function. Semin Cell Dev Biol 2007;18:332-339.

16 Chan YW, van den Berg HA, Moore JD, Quenby S, Blanks AM: Assessment of myometrial transcriptome changes associated with spontaneous human labour by high-throughput RNA-seq. Exp Physiol 2014;99:510-524.

17 Anderson NC, Ramon F, Snyder A: Studies on Calcium and Sodium in Uterine Smooth Muscle Excitation under Current-Clamp and Voltage-Clamp Conditions. J Gen Physiol 1971;58:322-339.

18 Anderson NC, Jr.: Voltage-clamp studies on uterine smooth muscle. J Gen Physiol 1969;54:145-165.

KARGER

19   Kao CY, Zakim D, Bronner F: Sodium influx and excitation in uterine smooth muscle. Nature 1961;192:1189-1190.

20   Kleinhaus AL, Kao CY: Electrophysiological actions of oxytocin on the rabbit myometrium. J Gen Physiol 1969;53:758-780.

21   Miyoshi H, Yamaoka K, Garfield RE, Ohama K: Identification of a non-selective cation channel current in myometrial cells isolated from pregnant rats. Pflugers Arch 2004;447:457-464.

22   Phillippe M, Basa A: Effects of sodium and calcium channel blockade on cytosolic calcium oscillations and phasic contractions of myometrial tissue. J Soc Gynecol Investig 1997;4:72-77.

23   Miller SM, Garfield RE, Daniel EE: Improved propagation in myometrium associated with gap junctions during parturition. Am J Physiol 1989;256:C130-141.

24   Seda M, Pinto FM, Wray S, Cintado CG, Noheda P, Buschmann H, Candenas L: Functional and molecular characterization of voltage-gated sodium channels in uteri from nonpregnant rats. Biol Reprod 2007;77:855-863.

25   Lu B, Su Y, Das S, Liu J, Xia J, Ren D: The Neuronal Channel NALCN Contributes Resting Sodium Permeability and Is Required for Normal Respiratory Rhythm. Cell 2007;129:371-383.

26   Lutas A, Lahmann C, Soumillon M, Yellen G: The leak channel NALCN controls tonic firing and glycolytic sensitivity of substantia nigra pars reticulata neurons. Elife 2016;5 e15271.

27   Flourakis M, Kula-Eversole E, Hutchison AL, Han TH, Aranda K, Moose DL, White KP, Dinner AR, Lear BC, Ren D, Diekman CO, Raman IM, Allada R: A Conserved Bicycle Model for Circadian Clock Control of Membrane Excitability. Cell 2015;162:836-848.

28   Gao S, Xie L, Kawano T, Po MD, Guan S, Zhen M, Pirri JK, Alkema MJ: The NCA sodium leak channel is required for persistent motor circuit activity that sustains locomotion. Nat Commun 2015;6:6323.

29   Reinl EL, Cabeza R, Gregory IA, Cahill AG, England SK: Sodium leak channel, non-selective contributes to the leak current in human myometrial smooth muscle cells from pregnant women. Mol Hum Reprod 2015;21:816-824.

30   Xin HB, Deng KY, Rishniw M, Ji G, Kotlikoff MI: Smooth muscle expression of Cre recombinase and eGFP in transgenic mice. Physiol Genomics 2002;10:211-215.

31   Pfaffl MW: A new mathematical model for relative quantification in real-time RT-PCR. Nucleic Acids Res 2001;29:e45.

32   Rosenbaum ST, Svalo J, Nielsen K, Larsen T, Jorgensen JC, Bouchelouche P: Immunolocalization and expression of small-conductance calcium-activated potassium channels in human myometrium. J Cell Mol Med 2012;16:3001-3008.

33   Zhu N, Eghbali M, Helguera G, Song M, Stefani E, Toro L: Alternative splicing of Slo channel gene programmed by estrogen, progesterone and pregnancy. FEBS Lett 2005;579:4856-4860.

34   Suresh A, Subedi K, Kyathanahalli C, Jeyasuria P, Condon JC: Uterine endoplasmic reticulum stress and its unfolded protein response may regulate caspase 3 activation in the pregnant mouse uterus. PLoS One 2013;8:e75152.

35   Floyd RV, Mobasheri A, Wray S: Gestation changes sodium pump isoform expression, leading to changes in ouabain sensitivity, contractility, and intracellular calcium in rat uterus. Physiol Rep 2017;5;e13527.

36   McLean AC, Valenzuela N, Fai S, Bennett SA: Performing vaginal lavage, crystal violet staining, and vaginal cytological evaluation for mouse estrous cycle staging identification. J Vis Exp 2012:e4389.

37   Kim BJ, Chang IY, Choi S, Jun JY, Jeon JH, Xu WX, Kwon YK, Ren D, So I: Involvement of Na$^+$-leak channel in substance P-induced depolarization of pacemaking activity in interstitial cells of Cajal. Cell Physiol Biochem 2012;29:501-510.

38   Wetendorf M, DeMayo FJ: Genetic engineering of mice to investigate uterine function in early pregnancy; in Croy BA, Yamada AT, DeMayo FJ, Adamson SL (eds): The guide to investigation of mouse pregnancy. Amsterdam, Elsevier/AP, 2014, pp 315-330..

39   Mesiano S, Welsh TN: Steroid hormone control of myometrial contractility and parturition. Semin Cell Dev Biol 2007;18:321-331.

40   Shynlova O, Lee YH, Srikhajon K, Lye SJ: Physiologic uterine inflammation and labor onset: integration of endocrine and mechanical signals. Reprod Sci 2013;20:154-167.

41   Sundelacruz S, Levin M, Kaplan DL: Role of membrane potential in the regulation of cell proliferation and differentiation. Stem Cell Rev 2009;5:231-246.

42   Sinke AP, Caputo C, Tsaih SW, Yuan R, Ren D, Deen PM, Korstanje R: Genetic analysis of mouse strains with variable serum sodium concentrations identifies the Nalcn sodium channel as a novel player in osmoregulation. Physiol Genomics 2011;43:265-270.

43   Ruan YC, Chen H, Chan HC: Ion channels in the endometrium: regulation of endometrial receptivity and embryo implantation. Hum Reprod Update 2014;20:517-529.